JOURNAL OF GUIDANCE, CONTROL, AND DYNAMICS
Vol. 19, No. 4, July–August 1996

On-Orbit Thruster Calibration

Peter J. Wiktor
Engineering Arts, Seattle, Washington 98115

Significant errors in force and moment output as well as large control coupling forces can result if the attitude and translation control thrusters of a spacecraft are not calibrated properly. Thruster calibration is also important for estimating fuel usage so that spacecraft life can be accurately predicted. A general procedure to accurately determine the true relationship between the commanded and the actual force output of a set of thrusters is presented. This relationship is determined from data generated by a spacecraft while it is in orbit. The calibration is based on the Kalman filter estimator and is verified by a digital computer simulation of the Gravity Probe B spacecraft dynamics. Gravity Probe-B is an Earth orbiting gravitational physics experiment, which will test several aspects of Einstein's general relativity theory. A set of 18 proportional thrusters generate attitude control moments around three axes and translation control forces along three axes for full six-degree-of-freedom control. A total of 108 parameters are needed to characterize both the force and moment outputs of all 18 thrusters. The ability to calibrate these parameters to an accuracy of better than 1% rms is demonstrated.

I. Introduction

A. Related Literature

THERE has been very little written on the subject of on-orbit thruster calibration. In contrast, there is a very rich literature in the fields of on-orbit attitude determination and on-orbit identification of spacecraft structural modes. In the field of on-line thruster calibration, Wittig et al.[1] measured the microaccelerations caused by thruster firings on a communications satellite. Prickett and Hoang[2] addressed on-orbit thruster calibration applied to estimating fuel usage for spacecraft life expectancy prediction. Parvez[3] computed the disturbance torques resulting from plume impingement using data available from an operational GSTAR satellite. Dodds and Milne[4] presented a method for automatic on-orbit estimation of a critical parameter of a thruster's impulse transfer characteristic. Attention is restricted to a single, isolated axis. Tahk et al.[5] estimated the pitch and roll misalignment of the primary lift thruster of a hovering kinetic energy weapon using an extended Kalman filter. Alekseev et al.[6] used an observer-based technique to detect the failure of a thruster on an underwater robotic vehicle.

B. Motivation

Dodds and Milne[4] state that on-orbit thruster calibration "facilitates optimal control with regards to thruster lifetime, fuel consumption and pointing accuracy." Accurate calibration of the thrusters on the ground prior to flight is limited by various factors. Among these is the difficulty of maintaining a suitable vacuum [$<10^{-4}$ torr (Refs. 7 and 8)] in a vacuum chamber during thruster calibration while continuously discharging gas from the thrusters. It is also difficult to predict and establish during ground testing the exact temperature and pressure conditions under which the thrusters will operate while in orbit. The output direction of the thrust will not necessarily be concentric with the nozzle. Measuring the true direction of the output thrust is very difficult on the ground especially considering plume impingement, which will further affect the net direction of a thruster's force and moment outputs.[9]

C. Summary

Figure 1 summarizes the general on-orbit thruster calibration scheme. A known disturbance force $\boldsymbol{F}(k)$ is applied to the spacecraft at time k. This force together with an external disturbance force $\boldsymbol{v}(k)$ and the output from the thruster system $T_c(k)\boldsymbol{a}(k)$ act on the spacecraft, causing the displacement $\boldsymbol{p}^{d/n}(k)$. An attitude and translation control system sends commands $T_c(k)$ to the thrusters to minimize this displacement. The on-orbit thruster calibration system (below the dotted line in Fig. 1) uses the second time derivative $\ddot{\boldsymbol{p}}^{d/n}(k)$ of this residual displacement to calculate the calibration force, $\boldsymbol{F}_c(k) = \boldsymbol{F}(k) - m\ddot{\boldsymbol{p}}^{d/n}(k)$. The calibration force $\boldsymbol{F}_c(k)$ is compared to the output from the thrusters, $\boldsymbol{F}_c(k) = T_c(k)\boldsymbol{a}(k) + \boldsymbol{v}(k)$. This equation acts as the measurement equation for a Kalman filter to estimate the thruster coefficients $\hat{\boldsymbol{a}}(k)$.

In the next section the general requirements for on-orbit thruster calibration are discussed assuming the ideal condition that the calibration forces are known exactly. Then a model of the thruster

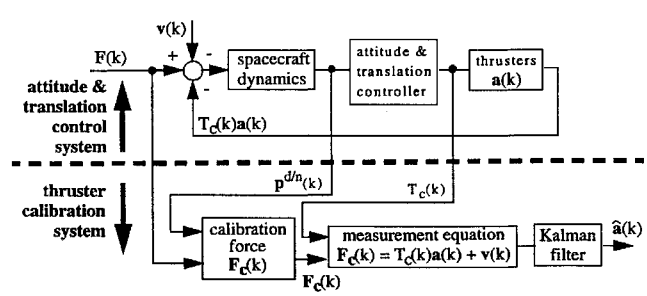

Fig. 1 On-orbit thruster calibration block diagram.

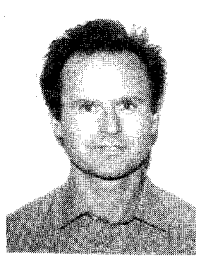

Peter J. Wiktor received his B.S. degree from the University of Pennsylvania in 1978, his M.S. degree from Rensselaer Polytechnic Institue in Troy, New York, in 1984, and his Ph.D. degree from Stanford University in 1992, all in Mechanical Engineering. He worked in flight test at McDonnell Douglas in Long Beach, California, from 1978 to 1980, traveled around the world in 1981, and worked at Hughes Helicopters in Los Angeles in 1981. From 1984 to 1987 as a Member of the Technical Staff at the Jet Propulsion Laboratory in Pasadena, California, Dr. Wiktor designed, developed, and tested momentum compensated reactionless precision pointing actuators for the Space Shuttle and interplanetary spacecraft. He is currently the President of Engineering Arts, a technology development company in Seattle, Washington.

Received April 25, 1994; revision received June 12, 1995; accepted for publication Jan. 28, 1996.

system is developed, which accounts for unknown disturbance forces, time-varying thruster coefficients, and thruster biases. A Kalman filter estimates the average value of the thruster coefficients in spite of these error sources. The Kalman filter requires knowledge of the process and measurement noise covariance matrices. A way to calculate these covariance matrices based on physical thruster system parameters is shown. Next, various techniques are discussed for generating known disturbance forces on a spacecraft, using Gravity Probe-B (GP-B)[10,11] as an example. These disturbances are designed to minimize thruster calibration errors resulting from unknown external disturbance forces, body fixed disturbance forces, and thruster biases. Finally, a verification of the on-orbit thruster calibration scheme via a digital computer simulation is discussed.

II. Calibration Technique

A. Problem Definition

The resulting force $\boldsymbol{F}_c$ on the spacecraft resulting from a set of thruster commands $\boldsymbol{T}_c$ is

$$\boldsymbol{F}_c = A\boldsymbol{T}_c \tag{1}$$

In general, $\boldsymbol{F}_c$ is a 6×1 vector composed of three components of force and three components of moment. The $n \times 1$ vector $\boldsymbol{T}_c$ is made up of the thrust commands to the n thrusters. The $6 \times n$ thruster configuration matrix A contains information on the output direction and magnitude of each thruster. The first three elements of the ith column of A give the magnitude and direction of the ith thruster's force output. Similarly the last three elements give the magnitude and direction of the moment output. The goal of thruster calibration is to identify the $6 \times n$ coefficients of A.

In the next subsection we define how many data are needed to calibrate the thrusters even under the ideal conditions of no measurement noise and no external disturbances. A general technique is developed in the subsequent subsection to calibrate the thrusters in spite of real world sensor noises, thruster biases, and external force disturbances.

B. Calibration Technique, No Noise

To calibrate the thrusters, a set of experiments, $k = 1, \ldots, m$, are performed. The number of experiments m required to calibrate the thrusters is addressed subsequently. In each experiment a calibration force $\boldsymbol{F}_c(k)$ is exerted on the spacecraft and the closed-loop spacecraft attitude and translation control system issues a set of thruster commands $\boldsymbol{T}_c(k)$ to compensate this disturbance. If the controller is working perfectly and there are no other disturbances on the spacecraft, then the thrusters exactly compensate the calibration force

$$\boldsymbol{F}_c(k) = A\boldsymbol{T}_c(k) \tag{2}$$

By performing m experiments with m different calibration forces, the following matrix relationship can be formed:

$$[\boldsymbol{F}_c(1), \ldots, \boldsymbol{F}_c(m)] = A[\boldsymbol{T}_c(1), \ldots, \boldsymbol{T}_c(m)] \tag{3}$$

Equation (3) is solved for A to calibrate the thrusters. The matrix $[\boldsymbol{T}_c(1), \ldots, \boldsymbol{T}_c(m)]$ must be square and full rank for A to exist and be unique. In this case A is given by

$$A = [\boldsymbol{F}_c(1), \ldots, \boldsymbol{F}_c(m)][\boldsymbol{T}_c(1), \ldots, \boldsymbol{T}_c(m)]^{-1} \tag{4}$$

A fundamental requirement that must be satisfied to calibrate the thrusters is stated as follows.

Requirement 2.1. To calibrate the thrusters, the thrust command vectors $\boldsymbol{T}_c(k)$ must span both the row space and null space of the thruster configuration matrix A. This is easy to see. The matrix A has n columns. If r_A is the rank of A, $\text{rank}(A) = r_A$, then the dimension of the row space is r_A and the dimension of the null space is $n - r_A$. The row space and null space of a matrix are orthogonal complements of each other.[12] As stated earlier, for A to exist and be unique matrix $[\boldsymbol{T}_c(1), \ldots, \boldsymbol{T}_c(m)]$ must be square, $m = n$, and full rank, $\text{rank}([\boldsymbol{T}_c(1), \ldots, \boldsymbol{T}_c(m)]) = n$. In other words, the vectors $\boldsymbol{T}_c(k), k = 1, \ldots, n$, must span the entire n dimensional input space of A. This means that they must span both the r_A dimensional row space as well as the $n - r_A$ dimensional null space of A.

The significance of Requirement 2.1 is that it explicitly defines the set of calibration forces $\boldsymbol{F}_c(k)$ and thruster commands $\boldsymbol{T}_c(k)$ required to calibrate the thrusters. Suppose that the pseudoinverse $A^\dagger$ of A is used for control[13]:

$$\boldsymbol{T}_c(k) = A^\dagger \boldsymbol{F}_c(k) \tag{5}$$

The resulting thruster commands $\boldsymbol{T}_c(k)$ are exclusively in the row space of A (Ref. 12). From this fact and Requirement 2.1, the following two important conclusions follow:

1) The calibration forces $\boldsymbol{F}_c(k)$ must span the entire column space of the thruster configuration matrix A. In physical terms this means that to calibrate the thrusters, calibration forces must be generated in all possible output directions of the thruster system. For a spacecraft with a full six-degree-of-freedom attitude and translation control system like GP-B, this means that independent calibration moments must be generated about the yaw, pitch, and roll axes and translation forces must also be generated along three mutually perpendicular axes. To see this, consider what happens if the calibration forces do not span the entire column space of A. In this case there exists a calibration force $\boldsymbol{F}_c(3)$, which is a linear combination of two other calibration forces,

$$\boldsymbol{F}_c(3) = \alpha_1 \boldsymbol{F}_c(1) + \alpha_2 \boldsymbol{F}_c(2) \tag{6}$$

Premultiplying Eq. (6) by $A^\dagger$ and using Eq. (5),

$$\boldsymbol{T}_c(3) = \alpha_1 \boldsymbol{T}_c(1) + \alpha_2 \boldsymbol{T}_c(2) \tag{7}$$

The thrust command vector $\boldsymbol{T}_c(3)$ is also a linear combination of two other thrust command vectors, $\boldsymbol{T}_c(1)$ and $\boldsymbol{T}_c(2)$. The matrix $[\boldsymbol{T}_c(1), \ldots, \boldsymbol{T}_c(m)]$ formed from these vectors, therefore, is not full rank and cannot be inverted to solve for A in Eq. (4).

2) Thruster commands $\boldsymbol{T}_n(k)$ in the null space of A are required to calibrate the thrusters. The null space of A is the set of all thruster commands $\boldsymbol{T}_n(k)$, which generate no output force, $A\boldsymbol{T}_n(k) = \boldsymbol{0}$. The pseudoinverse (5) does not generate any null space components $\boldsymbol{T}_n(k)$ (Ref. 12). To satisfy Requirement 2.1 these null space components $\boldsymbol{T}_n(k)$ must be added to the thruster control (5):

$$\boldsymbol{T}_c(k) = A^\dagger \boldsymbol{F}_c(k) + \boldsymbol{T}_n(k) \tag{8}$$

The null space components at different times k must be linearly independent so that the matrix, $[\boldsymbol{T}_c(1), \ldots, \boldsymbol{T}_c(m)]$ in Eq. (4) can be inverted.

In physical terms generating null space commands is equivalent to calibrating the thrusters against each other. Even though the null space commands do not produce an external output force, they do push and pull against each other and useful information for thruster calibration is obtained. Theoretically, there is no limit to the number of thrusters that can be calibrated using this scheme.

C. Calibration Technique, with Noise

The following assumptions were made in the preceding subsection.

1) The calibration force $\boldsymbol{F}_c(k)$ is known exactly.

2) The calibration force is the only force exerted on the spacecraft.

3) The closed-loop attitude and translation control system commands the thrusters to perfectly cancel the calibration force.

4) The thruster coefficients do not change with time. In other words, A is constant.

5) There are no thruster biases.

6) There are no body-fixed forces acting on the spacecraft. For example, if the spacecraft is spinning, then the mass properties must be balanced about the spin axis.

Naturally, none of these assumptions is valid in the real world. A more realistic model is developed in this section. This model is used to develop a calibration technique that can calibrate the thrusters in spite of sensor noise, disturbance forces, unmodeled mass offsets, and thruster biases.

To account for errors, recast Eq. (3) as a state estimation problem with the measurement equation

$$\boldsymbol{F}_c(k) = T_c(k)\boldsymbol{a}_w(k) + \boldsymbol{v}_m(k) + \boldsymbol{b} \tag{9}$$

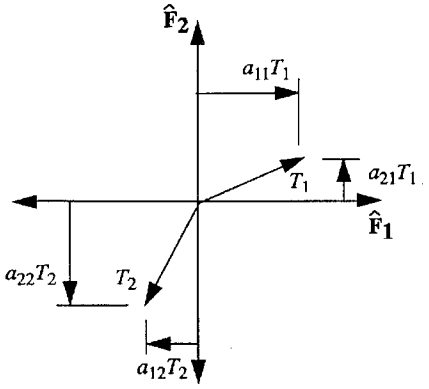

Fig. 2 Simple planar configuration of two thrusters.

The coefficients in the matrix A are now strung out into the vector $\boldsymbol{a}_w(k)$, and the thrust command vector $\boldsymbol{T}_c(k)$ is formed into the matrix $T_c(k)$. The measurement noise $\boldsymbol{v}_m(k)$ accounts for external disturbances on the spacecraft as well as errors in measuring the calibration force $\boldsymbol{F}_c(k)$. The vector $\boldsymbol{b}$ accounts for steady-state disturbances on the spacecraft resulting from thruster biases and unmodeled mass offsets. The components of the vector $\boldsymbol{a}_w(k)$ are time-varying thruster coefficients. Section II.D discusses various ways of generating calibration forces that minimize $\boldsymbol{v}_m(k)$ and $\boldsymbol{b}$.

To illustrate how to convert the thruster coefficients from a matrix A as in Eq. (2) into a vector $\boldsymbol{a}_w(k)$ as in Eq. (9), consider the simple thruster configuration depicted in Fig. 2, which consists of two thrusters in a plane. In matrix form the output force is given by

$$\boldsymbol{F}_c = A\boldsymbol{T}_c \tag{10}$$

$$\boldsymbol{F}_c = \begin{bmatrix} a_{11} & a_{12} \\ a_{21} & a_{22} \end{bmatrix} \begin{bmatrix} T_1 \\ T_2 \end{bmatrix} \tag{11}$$

and in vector form

$$\boldsymbol{F}_c = T_c\boldsymbol{a}_w \tag{12}$$

$$\boldsymbol{F}_c = \begin{bmatrix} T_1 & 0 & T_2 & 0 \\ 0 & T_1 & 0 & T_2 \end{bmatrix} \begin{bmatrix} a_{11} \\ a_{21} \\ a_{12} \\ a_{22} \end{bmatrix} \tag{13}$$

Notice that the elements of $\boldsymbol{a}_w$ are the columns of A stacked on top of each other.

The vectors $\boldsymbol{a}_w(k)$ in Eq. (9) are time-varying thruster coefficients. These are modeled as a mean value $\boldsymbol{a}$ plus a zero mean white process noise $\boldsymbol{w}(k)$:

$$\boldsymbol{a}_w(k) = \boldsymbol{a} + \boldsymbol{w}(k) \tag{14}$$

Substituting Eq. (14) into Eq. (9) results in the following measurement equation:

$$\boldsymbol{F}_c(k) = T_c(k)\boldsymbol{a} + \boldsymbol{v}(k) \tag{15}$$

The measurement noise $\boldsymbol{v}(k)$

$$\boldsymbol{v}(k) \overset{\text{def}}{=} T_c(k)\boldsymbol{w}(k) + \boldsymbol{v}_m(k) + \boldsymbol{b} \tag{16}$$

now accounts for variations in the thruster coefficients $\boldsymbol{w}(k)$, as well as the original measurement noise $\boldsymbol{v}_m(k)$ and thruster biases $\boldsymbol{b}$. Assuming $\boldsymbol{v}_m(k)$ and $\boldsymbol{w}(k)$ are uncorrelated, the covariance of $\boldsymbol{v}(k)$ is

$$V(k) \overset{\text{def}}{=} E\{[\boldsymbol{v}(k)-\boldsymbol{b}][\boldsymbol{v}(k)-\boldsymbol{b}]'\} = T_c(k)W(k)T_c'(k) + V_m(k) \tag{17}$$

where $W(k)$ is the covariance of $\boldsymbol{w}(k)$ and $V_m(k)$ is the covariance of $\boldsymbol{v}_m(k)$.

The goal of thruster calibration is to estimate the mean values $\boldsymbol{a}$ of the true thruster coefficients $\boldsymbol{a}_w(k)$. Since the mean values do not change with time, they can be modeled by the state equation

$$\boldsymbol{a} \overset{\text{def}}{=} \boldsymbol{a}(k+1) = \boldsymbol{a}(k) \tag{18}$$

The thruster calibration problem can now be stated as follows: given the state equation (18) together with the measurement equation (15), estimate the mean values of the thruster coefficients $\boldsymbol{a}$. A solution is the Kalman filter, which in this case reduces to weighted recursive least squares because of the time invariant state equation (18). From the Kalman filter, the state estimate $\hat{\boldsymbol{a}}$ is given by

$$\hat{\boldsymbol{a}}(k+1) = \hat{\boldsymbol{a}}(k) + K(k)[\boldsymbol{F}_c(k) - T_c(k)\hat{\boldsymbol{a}}(k)] \tag{19}$$

where the Kalman gain $K(k)$ is

$$K(k) = M(k)T_c(k)[V(k) + T_c(k)M(k)T_c'(k)]^{-1} \tag{20}$$

and the estimation error covariance matrix $M(k)$ is

$$M(k+1) = M(k) - K(k)T_c(k)M(k) \tag{21}$$

Notice that Eq. (20) involves the inversion of a matrix that is the same size as the measurement noise covariance matrix $V(k)$. This matrix is at most 6×6 in this case. This is one of the main advantages of implementing the calibration technique recursively. A batch least squares approach involves the inversion of a much larger matrix.

The rate of convergence of the Kalman filter depends on the proper choice of the process and measurement noise covariance matrices, $W(k)$ and $V(k)$. For optimal convergence, the values of $W(k)$ and $V(k)$ used in the filter should match the actual covariances of these noises. How to properly choose $W(k)$ and $V(k)$ is discussed next.

1. Process Noise Covariance Matrix, $W(k)$

Recall from Eq. (14) that at any time k the true thruster coefficients $\boldsymbol{a}_w(k)$ can vary from their mean values $\boldsymbol{a}$ by some zero mean process noise $\boldsymbol{w}(k)$. In this section it is shown how to estimate the covariance $W(k) \overset{\text{def}}{=} E\{\boldsymbol{w}(k)\boldsymbol{w}'(k)\}$ of this noise.

The easiest way to characterize variations $\boldsymbol{w}(k)$ in the thruster's coefficients is in terms of variations in scale factor $\Delta s(k)$ and angle $\Delta\boldsymbol{\theta}(k)$. For example, consider a thruster that nominally has a unit scale factor as depicted by the unit vector $\hat{\boldsymbol{a}}$ in Fig. 3. The true thruster output at time k is the vector $\boldsymbol{a}_w(k)$. It varies from the nominal value by the variation $\boldsymbol{w}(k)$. In terms of the components along the unit vectors $\hat{t}_1, \hat{t}_2, \hat{t}_3$ in the thruster frame, Eq. (14) is

$$\boldsymbol{a}_w(k) = \hat{\boldsymbol{a}} + \boldsymbol{w}(k) \tag{22}$$

$${}^t\boldsymbol{a}_w(k) = \begin{bmatrix} 1 \\ 0 \\ 0 \end{bmatrix} + \begin{bmatrix} {}^tw_1(k) \\ {}^tw_2(k) \\ {}^tw_3(k) \end{bmatrix} \tag{23}$$

The superscript t denotes that the components are written relative to the t frame, which is a local thruster frame, with $\hat{t}_1$ in the direction of the nominal thruster output $\hat{\boldsymbol{a}}$ and with $\hat{t}_2$ and $\hat{t}_3$ perpendicular to $\hat{t}_1$. Note that the nominal thruster output $\hat{\boldsymbol{a}}$ in Eq. (23) has unit magnitude.

Each of the components of ${}^t\boldsymbol{w}(k)$ in Eq. (23) is a function of either scale factor variations $\Delta s(k)$ or angle variations $\Delta\theta_2(k)$, $\Delta\theta_3(k)$:

$$\begin{bmatrix} {}^tw_1(k) \\ {}^tw_2(k) \\ {}^tw_3(k) \end{bmatrix} = \begin{bmatrix} \Delta s(k) \\ \Delta\theta_2(k) \\ \Delta\theta_3(k) \end{bmatrix} \tag{24}$$

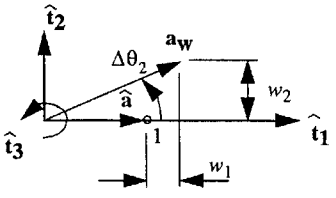

Fig. 3 Scale factor variations, $\Delta s(k)$, and angle variations, $\Delta\theta(k)$, of the outputs of the thrusters.

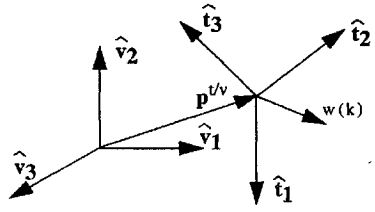

Fig. 4 Nominal thruster frame t, for a thruster is located at position $p^{t/v}$ relative to the vehicle frame v; vector w (k) represents the variation in magnitude and direction of the true output of the thruster from the nominal output.

The variation in scale factor $\Delta s(k)$ is defined as the amount that the magnitude of $\boldsymbol{a}_w(k)$ varies from unity, $\Delta s(k) \stackrel{\text{def}}{=} \|\boldsymbol{a}_w(k)\|_2 - 1$.

The significance of Eq. (24) is that it allows the variations in the thruster coefficients $\boldsymbol{w}(k)$ to be expressed in terms of parameters $\Delta s(k)$, $\Delta\theta_2(k)$, and $\Delta\theta_3(k)$, which have physical meaning. The variations in thruster scale factor $\Delta s(k)$ can be a result of variations in temperature, pressure, or specific impulse. The angle variations $\Delta\theta_2(k)$ and $\Delta\theta_3(k)$ can be a result of thruster misalignments, nonconcentric flow through the thruster nozzle, or plume impingement.[9]

If the scale factor and angle variations are uncorrelated, which is a good assumption, then the covariance of ${}^t\boldsymbol{w}(k)$ in the thruster frame is

$$ {}^tW(k) \stackrel{\text{def}}{=} E\{{}^t\boldsymbol{w}(k){}^t\boldsymbol{w}'(k)\} = \begin{bmatrix} \Delta s^2(k) & 0 & 0 \\ 0 & \Delta\theta_2^2(k) & 0 \\ 0 & 0 & \Delta\theta_3^2(k) \end{bmatrix} \tag{25} $$

Before ${}^tW(k)$ can be used in Eq. (17) and, subsequently, Eq. (20) for thruster calibration it must first be rotated to the vehicle frame (spacecraft reference frame). The rest of this subsection describes how to rotate a covariance matrix from one reference frame to another. The vector $\boldsymbol{w}(k)$ is depicted in Fig. 4, along with the vehicle frame, superscript v, and thruster frame, superscript t. If $\boldsymbol{w}(k)$ is written relative to the thruster frame ${}^t\boldsymbol{w}(k)$, then its components relative to the vehicle frame ${}^v\boldsymbol{w}(k)$ are given by the following coordinate transformation:

$$ {}^v\boldsymbol{w}(k) = {}^vS^t\,{}^t\boldsymbol{w}(k) \tag{26} $$

where ${}^vS^t$ is the coordinate transformation matrix from frame t to frame v. The covariance matrix ${}^vW(k)$ written relative to frame v therefore is

$$ {}^vW(k) \stackrel{\text{def}}{=} E\{{}^v\boldsymbol{w}(k){}^v\boldsymbol{w}'(k)\} = {}^vS^t\,{}^tW(k)\,{}^tS^v \tag{27} $$

$$ {}^vW(k) = {}^vS^t\,{}^tW(k)\,{}^tS^v \tag{28} $$

where ${}^tS^v$ is the transpose of ${}^vS^t$, ${}^tS^v = ({}^vS^t)'$. The covariance ${}^tW(k)$ transforms to ${}^vW(k)$ by a similarity transformation.

The coordinate transformation matrix ${}^vS^t$ must be formed before Eq. (28) can be used to rotate a covariance matrix from frame t to frame v. The columns of ${}^vS^t$ are the unit vectors $\hat{t}_1, \hat{t}_2, \hat{t}_3$ written in the v frame, ${}^vS^t \stackrel{\text{def}}{=} [{}^v\hat{t}_1\ {}^v\hat{t}_2\ {}^v\hat{t}_3]$. From Fig. 3, ${}^v\hat{t}_1$ is in the direction of the nominal thruster output direction $\hat{\boldsymbol{a}}$. Since $\hat{\boldsymbol{a}}$ has unit magnitude,

$$ {}^v\hat{t}_1 = {}^v\hat{\boldsymbol{a}} = \begin{bmatrix} {}^va_1 \\ {}^va_2 \\ {}^va_3 \end{bmatrix} \tag{29} $$

The other two columns in ${}^vS^t$, vectors $\hat{t}_2$ and $\hat{t}_3$, must be perpendicular to $\hat{t}_1$ and to each other. If a_1 and a_2 are not zero, then let

$$ {}^v\hat{t}_2 \stackrel{\text{def}}{=} \frac{1}{\sqrt{a_1^2 + a_2^2}} \begin{bmatrix} -a_2 \\ a_1 \\ 0 \end{bmatrix} \tag{30} $$

$$ {}^v\hat{t}_3 \stackrel{\text{def}}{=} {}^v\hat{t}_1 \times {}^v\hat{t}_2 \tag{31} $$

Notice that ${}^v\hat{t}_1\ {}^v\hat{t}_2\ {}^v\hat{t}_3$ in Eqs. (29–31) are perpendicular since they satisfy ${}^v\hat{t}_1 \cdot {}^v\hat{t}_2 = \boldsymbol{0}$, ${}^v\hat{t}_1 \cdot {}^v\hat{t}_3 = \boldsymbol{0}$, and ${}^v\hat{t}_2 \cdot {}^v\hat{t}_3 = \boldsymbol{0}$.

Thus far it has been shown how to generate the covariance matrix ${}^vW(k)$ for the force output of a thruster. But what about the moment output? This can be found by taking the cross product, $\boldsymbol{p}^{t/v} \times {}^v\boldsymbol{w}(k)$, between the location of the thruster $\boldsymbol{p}^{t/v}$ (Fig. 4) and the process noise ${}^v\boldsymbol{w}(k)$. If the cross product matrix $P^{t/v}$ is defined as

$$ P^{t/v} \stackrel{\text{def}}{=} \begin{bmatrix} 0 & -p_3^{t/v} & p_2^{t/v} \\ p_3^{t/v} & 0 & -p_1^{t/v} \\ -p_2^{t/v} & p_1^{t/v} & 0 \end{bmatrix} \tag{32} $$

so that $P^{t/v}\,{}^v\boldsymbol{w}(k) = \boldsymbol{p}^{t/v} \times {}^v\boldsymbol{w}(k)$, then the full 6×6 force and moment process noise covariance matrix is

$$ {}^vW_{6\times6}(k) \stackrel{\text{def}}{=} E\left\{ \begin{bmatrix} {}^v\boldsymbol{w}(k) \\ P^{t/v}\,{}^v\boldsymbol{w}(k) \end{bmatrix} [{}^v\boldsymbol{w}'(k) \quad {}^v\boldsymbol{w}'(k)(P^{t/v})'] \right\} $$

$$ = \begin{bmatrix} {}^vW(k) & {}^vW(k)(P^{t/v})' \\ P^{t/v}\,{}^vW(k) & P^{t/v}\,{}^vW(k)(P^{t/v})' \end{bmatrix} \tag{33} $$

A small perturbation can be added to Eq. (33) to keep ${}^vW_{6\times6}(k)$ from being singular.

To summarize, in this subsection it has been shown how to express the process noise covariance matrix ${}^vW_{6\times6}(k)$ of a thruster in terms of parameters that have physical meaning: scale factor error $\Delta s(k)$, angle error $\Delta\theta(k)$, thruster location $\boldsymbol{p}^{t/v}$, and nominal thruster output $\hat{\boldsymbol{a}}$. How to rotate a covariance matrix from one reference frame to another through a similarity transformation has also been discussed.

2. *Measurement Noise Covariance Matrix, $V(k)$*

The measurement noise $\boldsymbol{v}_m(k)$ in Eq. (9) accounts for uncertainty in the calibration force $\boldsymbol{F}_c(k)$, as well as any unmodeled external disturbances acting on the spacecraft. The covariance of this noise, $V_m(k)$, therefore depends on the specific way in which the calibration forces are generated. Several ways of generating calibration forces and reducing the measurement noise $\boldsymbol{v}_m(k)$ are described in the next subsection.

D. Generating Calibration Forces

The way that calibration forces are generated for on-orbit thruster calibration depends on the specific actuators and sensors installed on the spacecraft. The GP-B spacecraft, for example, has an independent mass trim control system used for mass balancing but which can be displaced a known amount to generate calibration forces. The thrusters are calibrated against these kinds of calibration forces in the simulation verification (Sec. III). Various averaging, differencing, and filtering techniques are used on GP-B to generate calibration forces that result in the best possible thruster calibration. Although these techniques are applied to a spacecraft with a mass trim system (or any independently movable mass), they can be applied to calibrate the thrusters on any spacecraft in general. If a spacecraft does not have a mass trim system, for example, then calibration forces can be generated by sending oscillating commands to the thrusters. The calibration forces in this case are calculated from the resulting spacecraft displacements measured by the attitude and translation control system sensors.

The external disturbances on the spacecraft resulting from aerodynamic drag and other effects can be quite large compared to the calibration forces. Based on simulations it was found that initially the calibration algorithm converges rapidly and then levels off (Fig. 5). Loosely speaking, the calibration levels off at an accuracy comparable to the relative magnitude of the unmodeled external disturbance force. To calibrate the thrusters to 1% of peak thrust in a reasonable length of time, for example, the magnitude of the external disturbance force must also be about 1% of peak thrust. Arbitrarily small calibration accuracies are theoretically possible given enough data, time, and averaging to do the calibration.

The GP-B spacecraft (Fig. 6) rolls slowly (one revolution every 10 min) about the longitudinal axis. Centrifugal forces and moments

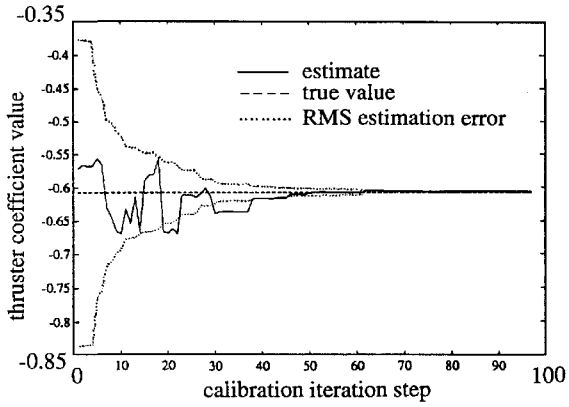

Fig. 5 Calibration convergence without aerodynamic drag of a typical thruster coefficient.

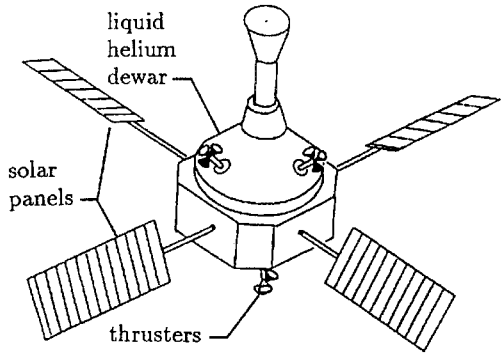

Fig. 6 GP-B spacecraft with solar panels and thrusters.

can be generated on the spacecraft by offsetting the center of mass and a principal axis of inertia of the spacecraft away from this axis with the mass trim system. Only four calibration forces can be generated with these static experiments: two translation forces normal to the roll axis and pitch and yaw moments. To satisfy Requirement 2.1 so that the thrusters can be calibrated, translation forces along the roll axis and roll moments must also be generated. These are generated by dither experiments, where the mass trim system is sinusoidally dithered along and around the roll axis. The two types of calibration forces, static and dither, are outlined in the next two subsections.

1. Dither Experiments

For small displacements of the mass trim system, the acceleration of the spacecraft $\ddot{\boldsymbol{p}}^{d/n}$ relative to inertial space times the mass of the spacecraft, $(m_D + m_R)$, equals the forces applied to the spacecraft by the thrusters $T_c\boldsymbol{a}$, the mass trim system $-m_R\ddot{\boldsymbol{p}}^{r/d}$, and external disturbances $\boldsymbol{v}$:

$$(m_D + m_R)\ddot{\boldsymbol{p}}^{d/n} = T_c\boldsymbol{a} - m_R\ddot{\boldsymbol{p}}^{r/d} + \boldsymbol{v} \tag{34}$$

where $\ddot{\boldsymbol{p}}^{r/d}$ is the acceleration of the mass trim system relative to the main body of the spacecraft and $\boldsymbol{v}$ accounts for unmodeled disturbances. In Eq. (34), m_D and m_R are the mass of the main body of the spacecraft and the mass trim system, respectively. By rearranging terms, Eq. (34) can be written in our standard measurement equation form, Eq. (9), with calibration force

$$\boldsymbol{F}_c \stackrel{\text{def}}{=} (m_D + m_R)\ddot{\boldsymbol{p}}^{d/n} + m_R\ddot{\boldsymbol{p}}^{r/d} \tag{35}$$

Given a sinusoidal dither of the mass trim system at a frequency of ω_d, the amplitude of the accelerations $|\ddot{\boldsymbol{p}}^{d/n}|$ and $|\ddot{\boldsymbol{p}}^{r/d}|$ can be determined from the position amplitudes $|\boldsymbol{p}^{d/n}|$ and $|\boldsymbol{p}^{r/d}|$ as follows:

$$|\ddot{\boldsymbol{p}}^{d/n}| = |\boldsymbol{p}^{d/n}|\omega_d^2 \qquad |\ddot{\boldsymbol{p}}^{r/d}| = |\boldsymbol{p}^{r/d}|\omega_d^2 \tag{36}$$

Table 1 Thruster calibration simulation parameters

Parameter	Value
Spacecraft mass, kg	$m_D = 2000$
Spacecraft inertia, kg · m^2	$I^{D/d} = \text{diag}(1077, 1077, 1185)$
Mass trim mass, kg	$m_R = 50$
Mass trim inertia, kg · m^2	$I^{R/r} = \text{diag}(39, 39, 78)$
Spacecraft roll frequency, rad/s	$\omega_3 = 2\pi/600$
Spacecraft orbit frequency, rad/s	$wo = 2\pi/(97.7 \times 60)$
Mass trim trans. dither freq., rad/s	$\omega_d = 10\omega_3$
Mass trim roll dither freq., rad/s	$\omega_d = 2.5\omega_3$
Attitude control bandwidth, rad/s	3
Translation control bandwidth, rad/s	0.5
Roll control bandwidth, rad/s	0.06
Control sample time, s	$T_s = 1$
Peak aerodynamic drag, mN	0.1

To accurately calculate the amplitude of the accelerations in Eq. (36), it is necessary to pick out the amplitudes of the spacecraft and mass trim motions $|\boldsymbol{p}^{d/n}|$ and $|\boldsymbol{p}^{r/d}|$ at the dither frequency ω_d from data that are corrupted by sensor noise and external disturbances. Use synchronous demodulation to zoom in on the amplitudes specifically at dither frequency. Synchronous demodulation and its subsequent low-pass filtering is equivalent to the discrete Fourier transform $z(w_d)$ of a time-domain signal $z(qT_s)$ at a specific frequency w_d:

$$z(w_d) \stackrel{\text{def}}{=} \frac{1}{n}\sum_{q=1}^{n} z(qT_s)\exp[-(i\omega_d qT_s)] \tag{37}$$

The variable T_s in Eq. (37) is the sample frequency, and n is the number of samples of the signal $z(qT_s)$. In the simulation verification (Sec. III), the mass trim system was dithered for at least 10 cycles before doing the synchronous demodulation.

The dither frequency ω_d must be chosen carefully to minimize measurement noise. It should be well below the translation and attitude control system bandwidths so that these control systems have enough time to compensate the disturbances caused by the mass trim system. The dither frequency must not coincide with any other disturbance frequency or structural mode and it must be high enough to produce a large enough calibration signal. Taking these considerations into account, the mass trim translation and roll dither frequencies listed in Table 1 were chosen.

The output from each thruster nozzle is one sided; therefore, it cannot go negative. To get a full sine wave command signal for each thruster, a steady state dc offset is commanded to its opposing pair. If the magnitude of the offset is bigger than the largest thruster command, then control can be done with only one nozzle out of a pair.

2. Static Experiments

Averaging techniques are used to reduce the effect of external disturbance forces on thruster calibration. The mass trim system is offset and held there for at least one complete orbit. The thrusters compensate the forces produced by this offset as well as the external disturbance forces. The average thruster command over the orbit is used for thruster calibration. The average body fixed external disturbance is much smaller than a typical instantaneous external disturbance. Since the average thruster commands compensate the average external disturbance, the effects of external disturbances are diminished dramatically.

To get rid of possible thruster calibration errors resulting from body fixed disturbance forces and thruster biases, the mass trim system is displaced to two separate positions and the calibration force is defined as the difference between the resulting two centrifugal forces.

For an in depth discussion of this technique and of static calibration in general, see Ref. 14.

III. Simulation

Verification of the calibration technique was done using two separate computer programs. The dynamics of the spacecraft are simulated using a Fortran program written by Jafry.[9] The thrusters are then calibrated in a MATLAB[15] program written by the author.

Crifasi[16] and Adachi[17] also contributed to the Fortran and MATLAB programs.

Jafry's program is a full six-degree-of-freedom nonlinear simulation of the spacecraft dynamics. It incorporates closed-loop attitude and translation control systems, as well as an independent mass trim system. The mass trim system can be moved in the simulation to induce calibration forces on the spacecraft. Sensor noises, thruster noises, thruster biases, mass properties offsets, and external disturbances can all be added to the simulation to determine their effects on thruster calibration.

To calibrate the thrusters the mass trim system is moved to various positions and dithered at various amplitudes and frequencies. The resulting spacecraft motions and thruster commands are sent to the MATLAB calibration program, which automatically sorts and processes the data yielding an estimate of the thruster coefficients.

The GP-B thruster system used in the simulation consists of 18 thrusters arranged in groups of 3 on the 6 faces of a cube. Nine of these thrusters are visible in Fig. 6. The locations, pointing directions, and scale factors of the thrusters were perturbed by roughly 10% from their nominal values. The on-orbit thruster calibration scheme developed in this article was used to estimate the force and moment output (6 coefficients) of each of the 18 thrusters for a total of $6 \times 18 = 108$ thruster coefficients. The parameters used for simulation are summarized in Table 1.

The simulation program was run with and without aerodynamic drag.

Without aerodynamic drag, after 96 experiments the estimated thruster coefficients converged to their true values with an error of 0.27% rms. The rms calibration error is defined as

$$(\text{rms})_{\text{error}} \stackrel{\text{def}}{=} \sqrt{\frac{1}{n}\sum_{i=1}^{n}(\hat{a}_i - a_i)^2}$$

where n is the number of thruster coefficients, a_i are the true thruster coefficients, and $\hat{a}_i$ are the estimates of those coefficients.

With aerodynamic drag, data for 48 experiments were obtained. With a peak drag level of 0.1 mN, the calibration converged with an error of 1.05%. The convergence rates with and without drag (Figs. 7 and 5) are almost identical. This means that with 96 experiments the calibration with drag would converge to roughly the same accuracy as the no drag calibration (0.27%).

Figure 8 is a three-dimensional plot of the thruster coefficient estimation errors, $a_i - \hat{a}_i$ $(i = 1, \ldots, 108)$, for all 108 thruster coefficients. This plot serves as a visual confirmation that the calibration algorithm does in fact converge on 108 individual thruster coefficients.

The six-degree-of-freedom simulation program in Fortran takes a long time to run. To generate enough data for 96 experiments to calibrate 108 coefficients takes approximately 5 h on an IRIS work station, which is roughly seven times faster than a SUN Sparc Station. Processing these data in MATLAB to calibrate the thrusters takes about 15 min.

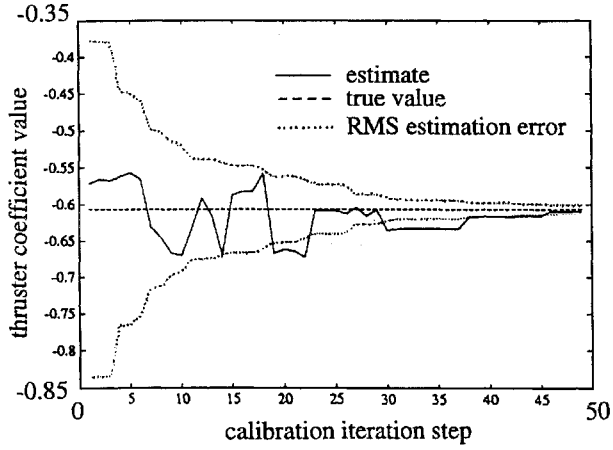

Fig. 7 Calibration convergence with aerodynamic drag of a typical thruster coefficient.

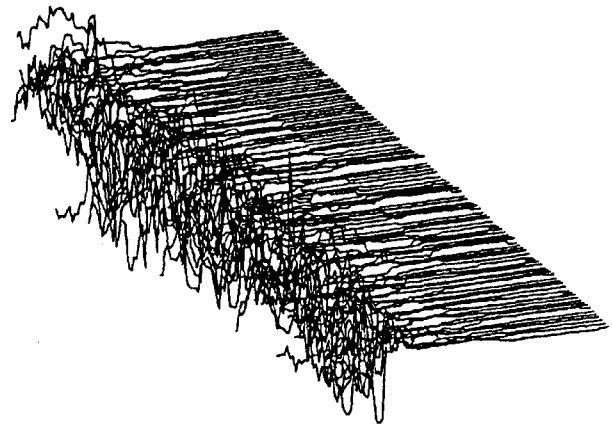

Fig. 8 Three-dimensional plot of thruster coefficient estimation errors, for all 108 coefficients. No aerodynamic drag.

IV. Impact on Spacecraft Operations

On-orbit thruster calibration can influence spacecraft design, operations, telemetry, attitude control, translation control, temperature control, thruster control, and on-orbit processing requirements. Here are two implications of on orbit thruster calibration.

A. Time

It takes at least five full days to gather enough data (96 experiments) to calibrate 18 thrusters (108 coefficients) to an accuracy of better than 1%. For each static experiment, the mass trim system must be moved and then the thruster commands must be averaged for at least 10 spacecraft roll periods, that is approximately one orbit period. At least 10 periods are required for each dither experiment. This takes 10 min for translational dither along the roll axis and 42 min for rotational dither around the roll axis.

B. Data

It takes at least 17.3 MB of data to calibrate 108 thruster coefficients to an accuracy of better than 1%. The data are sampled every second to avoid aliasing the control signals caused by the response of the spacecraft to atmospheric density variations, which are expected to have a magnitude of 10% of the nominal drag level at a frequency of 0.1 Hz. By doing some on-orbit data processing, the amount of data that has to be sent down to the ground via telemetry reduces to 6.2 kB. The on-orbit processing involves time averaging for static experiments and synchronous demodulation for dither experiments.

V. Summary

The following is a summary of the major developments of this article.

A. General Requirements

Calibration forces must be generated in all possible output directions of the thruster system, and null space thruster commands must be generated to fully calibrate the set of thrusters. Adding null space thruster commands causes the thrusters to push and pull against each other allowing for self-calibration of the thrusters.

B. Thruster Model

A thruster model is developed that accounts for time-varying thruster coefficients, external disturbance forces, and measurement noise.

C. Kalman Filter

A Kalman filter-based estimation scheme is developed that does not depend on any specific way of generating calibration reference forces. The measurements from several different calibration experiments using a variety of different types of calibration forces can be concatenated into a single Kalman filter to estimate the thruster coefficients. The estimates of the thruster coefficients generated by the Kalman filter converge to the true values in spite of zero mean

disturbances, sensor noises, and steady-state biases. By adding fictitious process noise, the Kalman filter will track slowly time-varying thruster coefficients.

D. Calibration Forces

Various techniques of generating calibration forces are developed that minimize process and measurement noise. These techniques involve averaging, filtering (synchronous demodulation), and differencing.

E. Simulation Verification

The feasibility of on-orbit thruster calibration has been demonstrated using a digital computer simulation of the GP-B spacecraft dynamics. The ratio of output force and moment (6 coefficients) to the commanded output was determined to an accuracy of better than 1% rms for 18 individual thrusters (108 coefficients total). At least five full days and 17.3 MB of data are required to calibrate 18 thrusters to better than 1% accuracy.

Acknowledgments

The research was sponsored under NASA Grant NAS8-36125. The work was conducted at Hanson Laboratories, GP-B, Stanford University. The author wishes to acknowledge Yusuf Jafry for writing the computer simulation of the GP-B spacecraft and for numerous suggestions on thruster calibration. Dan DeBra must be acknowledged for originally suggesting on-orbit thruster calibration. Thanks are given to Thierry Crifasi for running the computer simulations.

References

[1]Wittig, M., van Holtz, L., Tunbridge, D. E. L., and Vermeulen, H. C., "In-Orbit Measurements of Microaccelerations of ESA's Communication Satellite OLYMPUS," *Proceedings of SPIE, International Society for Optical Engineering*, Munich, Germany, SPIE-90-112, 1990.

[2]Prickett, R. P., and Hoang, J. V., "Satellite Propulsion Performance Modelling Using Flight Data," *Journal of Propulsion and Power*, Vol. 8, No. 5, 1992, pp. 971–979.

[3]Parvez, S. A., "STAR Satellite Disturbances from Plume Impingement," *Journal of Spacecraft and Rockets*, Vol. 27, No. 3, 1990, pp. 275–278.

[4]Dodds, S. J., and Milne, P. A., "Automatic Gas-Jet Parameter Estimation for High Precision Spacecraft Attitude Control System," *Transactions of the Institute of Measurement and Control*, Vol. 10, No. 2, 1988.

[5]Tahk, M., Trikas, T., and Wallace, B., "Postflight Data-Reduction Techniques for Hovered Kinetic Energy Weapons," *Journal of Guidance, Control, and Dynamics*, Vol. 14, No. 5, 1991, pp. 872–877.

[6]Alekseev, Y. K., Kostenko, V. V., and Shumsky, A. Y., "Use of Identification and Fault Diagnostic Methods for Underwater Robotics," *OCEANS 94, Oceans Engineering for Today's Technology and Tomorrow's Preservation* (Brest, France), Oceanic Engineering Society, Vol. 2, Inst. of Electrical and Electronics Engineers, New York, 1994, pp. 489–494.

[7]Bull, J. S., "Precise Attitude Control of the Stanford Relativity Satellite," Ph.D. Thesis, Dept. of Aeronautics and Astronautics, Stanford Univ., SUDAAR 452, Stanford, CA, March 1973.

[8]Chen, J.-H., "Helium Thrustor Propulsion System for Precise Attitude Control and Drag Compensation of the Gravity Probe B Satellite," Ph.D. Thesis, Dept. of Aeronautics and Astronautics, Stanford Univ., SUDAAR 538, Stanford, CA, Dec. 1983.

[9]Jafry, Y. R., "Aeronomy Coexperiments on Drag-Free Satellites with Proportional Thrusters: GP-B and STEP," Ph.D. Thesis, Dept. of Aeronautics and Astronautics, Stanford Univ., SUDDAR 619, Stanford, CA, March 1992.

[10]Schiff, L. I., "Motion of a Gyroscope According to Einstein's Theory of Gravitation," *Proceedings of the National Academy of Sciences*, Vol. 46, No. 871, 1960, pp. 732–745.

[11]Turneaure, J. P., Everitt, C. W. F., and Parkinson, B. W., "The Gravity Probe B Relativity Gyroscope Experiment: Approach to a Flight Mission," *Proceedings of the 4th Marcel Grossman Meeting on General Relativity*, Rome, Italy, 1986.

[12]Strang, G., *Linear Algebra and Its Applications*, Harcourt Brace Jovanovich, San Diego, CA, 1989.

[13]Wiktor, P. J., and DeBra, D. B., "The Minimum Control Authority of a System of Actuators with Applications to Gravity Probe B," 14th Annual AAS Guidance and Control Conference, AAS Paper 91-026, Keystone, CO, 1991.

[14]Wiktor, P. J., "The Design of a Propulsion System Using Vent Gas from a Liquid Helium Cryogenic System," Ph.D. Thesis, Dept. of Aeronautics and Astronautics, Stanford Univ., SUDDAR 624, Stanford, CA, June 1992.

[15]Moler, C., Little, J., and Bangert, S., "Matlab User's Guide," MathWorks, Inc., Sherborn, MA, 1990.

[16]Crifasi, T., "On Orbit Thruster Calibration," M.S. Thesis, Dept. of Aeronautics and Astronautics, Stanford Univ., Stanford, CA, June 1991.

[17]Adachi, K., "Nonlinear on Orbit Thruster Calibration," Engineer's Thesis, Dept. of Aeronautics and Astronautics, Stanford Univ., Stanford, CA, Nov. 1992.